Radar cross section (RCS) of perfect electromagnetic conductor (PEMC) cylinder by a Laguerre–Gaussian beam

M. Arfan [1], A. Ghaffar [2, *], M.Y. Naz [3], M. A. Hanif [4]

[1, 2, 3] *Dept. of Physics, University of Agriculture, Faisalabad 38000, Pakistan.*
[4] *Dept. of Chemistry, University of Agriculture, Faisalabad 38000, Pakistan.*

Corresponding author: aghaffar16@uaf.edu.pk

Abstract

Radar Cross Section (RCS) of perfect electromagnetic conductor (PEMC) cylinder using an incident Laguerre–Gaussian (LG) beam has been investigated. LG beam potential function is used to expand the incident and scattered electromagnetic (EM) field components. The co- and cross-polarized scattered field coefficients are determined by applying the PEMC boundary conditions at the interface i.e., $r = a$. The obtained values for co- and cross-polarized scattered field components would be helpful to find out the scattered field distribution. A comparison of our results for PEMC and PMC for fundamental LG beam with beam mode $p = 0$, $l = 0$, i.e., LG_{00} match with the gaussian beam scattering as witnessed in published work. The effects of OAM mode index (l), beam waist radius (w_0), and PEMC cylinder radius on RCS have been analyzed.

Keywords: Cylinder; Laguerre–Gaussian (LG) beam; PEMC; PMC ;radar cross section (RCS).

1. Introduction

The concern of optical researchers towards Laguerre–Gaussian (LG) beam have increased due to its intrinsic differential field distribution and helical phase front which results transfer of angular momentum along with sensing of small-scale characteristics to the illuminated objects (Friese *et al*., 1996; Tempere *et al*., 2001; Mair *et al*., 2001). Beam with helical/twisted phased profile carrying orbital angular momentum (OAM) is well known for LG beam. The magnitude of OAM associated with each photon is characterized by $l\hbar$ term. The beam indices, p describes the node number of the beam radial profile and l stands for angular degree of freedom about the propagation direction. LG beam form remains stable for free space propagation i.e., scale of intensity profile in a cross-section changes but on the optical axis the zero intensity can be observed. Owing to this, such beams are also renowned for optical vortices (Yao and Padgett, 2011).

Recent works have focused on the LG beam scattering for different orders of OAM through several types of metamaterials such as PEMC sphere (Arfan *et al.*, 2022b) and chiral coated PEMC cylinder (Arfan *et al.*, 2022a) that are being widely used for various purposes. Furthermore, these beams are being used to estimate the RCS of scattered field for various shaped materials as, dielectric slab (Li *et al.*, 2017), complicated biological cells (Yu *et al.*, 2018), chiral particles (Cui *et al.*, 2021), and chiral sphere (Qu *et al.*, 2016).

The suggestion of generality of a perfect electric conductor (PEC) and perfect magnetic conductor (PMC) results in perfect electromagnetic conductor (PEMC) as proposed by (Sihvola, 2007) and this allows us to study the scattering of LG beam as a substitute for the extended waves infinitely using a PEMC cylinder. It has been seen that PEMC, PEC, and PMC differ in that the PEMC contains a supplementary cross-polarized field component. The well-defined boundary conditions at the surface of PEMC are

$$\boldsymbol{n} \times (\mathbf{H} + M\mathbf{E}) = 0$$
$$\boldsymbol{n} \cdot (\mathbf{D} - M\mathbf{B}) = 0 \tag{1}$$

Here, $\boldsymbol{n}$ is the unit normal and M is the admittance parameter of PEMC cylinder. The limiting values for admittance parameter as $M = 0$ and $M \to \pm\infty$, the PEMC becomes PMC and PEC respectively.

The study of interaction between EM waves and magnetized plasma slab is discussed to compute the reflection and transmission coefficients. Numerical results explore that reflectance can be tuned by adjusting the effective collision frequency and metallic substrate (Zhao and Xie, 2016). The problem of the scattering of EM radiation for PEMC sphere and PEMC cylinder was theoretically discussed by (Ruppin, 2006b; Ruppin, 2006a). The study related to PEMC scattering for different arrangements has been conducted by many researchers (Ahmed *et al.*, 2011; Ghaffar *et al.*, 2013; Lindell and Sihvola, 2005; Sihvola and Lindell, 2006). In this manuscript, the incident LG beam is expanded using LG potential function. However, the scattering characteristics of LG beam by a PEMC cylinder has not been considered in literature. So, scattering features of LG beam towards PEMC cylinder are treated. The interaction of PEMC cylinder by varying the LG beam order, beam waist, and cylinder radius on the scattered field is computed. The boundary conditions of the PEMC cylinder have been imposed to obtain the scattering field coefficients. In all the calculations, the field dependence for time factor i.e., $e^{-i\omega t}$ is assumed.

2. Description of the problem and governing equations

The geometry of our problem is depicted in Figure. 1. A PEMC cylinder is considered to study the interaction of LG beam. The radius of the cylinder is a with infinite length. The field polarizations are defined as, when the polarized incident field is parallel to the axis of PEMC cylinder, then it is called transverse magnetic (TM) polarization and when the polarized incident field becomes perpendicular to the cylinder axis then it is known as transverse electric (TE) polarization. For PEMC cylinder, the cross polarized TM component appears in the scattered field for an incident LG beam.
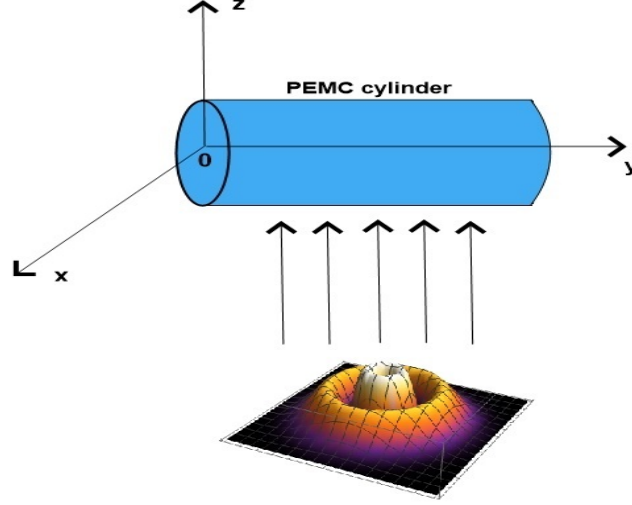
Fig. 1. Geometry of the scattering problem.

Now the LG beam is propagating along the z-axis and its potential with amplitude factor $\widetilde{V_0}$ in a cylindrical coordinate system is given as (Mendonca *et al.*, 2009; Shahzad and Ali, 2014; Ayub *et al.*, 2011),

$$V(r,t) = \widetilde{V_0}\, F_{pl}(r,z)\exp[i(l\varphi + kz - \omega t)] \tag{2}$$

The equation (2) tells that LG potential depends on mode numbers p, l, and azimuthal angle (φ) with helical phase structure through $\exp[i(l\varphi + kz - \omega t)]$ factor. In a cylindrical coordinate system (r, φ, z), the electric field components can be written as,

$$E_r = -\partial_r V(r,t) = -\frac{1}{F_{pl}}\frac{\partial F_{pl}}{\partial r}\,V(r,t) \tag{3}$$

$$E_\varphi = -\partial_\varphi V(r,t) = -\frac{il}{r}V(r,t) \tag{4}$$

$$E_z = -\partial_z V(r,t) = -\left(ik + \frac{1}{F_{pl}}\frac{\partial F_{pl}}{\partial z}\right)V(r,t) \tag{5}$$

where the LG mode function is defined as,

$$F_{pl}(r,z) = \frac{1}{2\sqrt{\pi}}\sqrt{\frac{(l+p)!}{p!}}\,(\mathrm{X})^{|l|}L_p^{|l|}(\mathrm{X})\exp\left(-\frac{\mathrm{X}}{2}\right) \tag{6}$$

where $\mathrm{X}=\frac{r^2}{w^2(z)}$ and $w(z) = w_0\sqrt{1 + \left(\frac{z}{z_R}\right)^2}$ be the beam width which turns to beam waist w_0 at $z = 0$. The term $z_R = \left(\frac{1}{2}\right)kw_0^2$ expresses the Rayleigh length. Beam parameters $(p\ \&\ l)$ denote radial and azimuthal index. $L_p^l(.)$ expresses the associated Laguerre polynomial.

For parallel polarized incident field, plugging equation (2) into equation (5), so

$$E_z^i = -\partial_z V(r,t) = -\left(ik + \frac{1}{F_{pl}}\frac{\partial F_{pl}}{\partial z}\right)\widetilde{V_0}\, F_{pl}(r,z)exp\,[i(l\varphi + k_0 z - \omega t)] \tag{7}$$

Now using equation (10) of (Kozaki, 1982) under special case i.e., on substituting $\alpha = 0$ and putting in equation (7) so the above mathematical expression for incident field can be modified as,

$$E_z^i = -\widetilde{V_0}\exp[i(l\varphi - \omega t)]\left(ik\, F_{pl} + \frac{\partial F_{pl}}{\partial z}\right)F_{pl}(r,z)\sum_{n=-\infty}^{\infty} j^n J_n(k_0 r)e^{in\varphi}\hat{z} \tag{8}$$

The scattered field can be expressed as,

$$E_z^s$$

$$= -\widetilde{V_0}\exp[i(l\varphi - \omega t)]\bigg(ik\, F_{pl}$$

$$+ \frac{\partial F_{pl}}{\partial z}\bigg)F_{pl}(r,z)\sum_{n=-\infty}^{\infty} j^n[a_n H_n^{(2)}(k_0 r)\hat{z} + b_n(\frac{in}{k_0 r}H_n^{(2)}(k_0 r)\hat{r} - H_n^{(2)\prime}(k_0 r)\hat{\varphi})]\,e^{in\varphi} \tag{9}$$

Where $J_n(.)$ and $H_n^{(2)}(.)$ are the Bessel functions of the 1st kind and Hankel functions of the 2nd kind, respectively. Prime denotes the derivative of the function with respect to the whole argument. In these expressions, a_n & b_n are the scattering coefficients of co- and cross-polarized field. The magnetic field components H_φ^i and H_φ^s can be known by using Maxwell's equations (Jackson, 1999) on the field equation (8-9).

To find out the unknown coefficients, the tangential and radial EM field components would satisfy the boundary conditions on the surface of the PEMC cylinder i.e., $r = a$ (Ruppin, 2006a) as,

$$H_t^{\ i} + ME_t^{\ i} + H_t^{\ s} + ME_t^{\ s} = 0 \tag{10}$$

$$\epsilon_0 E_r^{\ i} + \epsilon_0 E_r^{\ s} - M\mu_0 H_r^{\ i} - M\mu_0 H_r^{\ s} = 0 \tag{11}$$

On implementing the above-mentioned boundary conditions, the linear equations are obtained. These are solved simultaneously to determine the co- and cross polarized scattering field coefficients.

3. Results and discussion

The complete theoretical formulation is derived in Section 2 and its implementation into Mathematica program is done in Section 3. In this section, scattering characteristics of the PEMC cylinder illuminated by an LG beam is numerically presented. The source frequency is set at 1 GHz and beam waist radius is $w_0 = 1.0\,\lambda$. In Figure. 2, the radial component of the incident electric field at different z positions i.e., $z = z_R, 3z_R$, and $7z_R$ for LG_{01} beam is depicted. The top

Figure. 2a presents the distributions in a quite small area as compared to the remaining Figures. 2(b-c) respectively. It can be seen that for LG beam incidence, a broadening is noted with increasing the propagation distance. The LG electric field distributions lead to a twisted field type structure which gives a strong basis for helical LG beam oscillations.
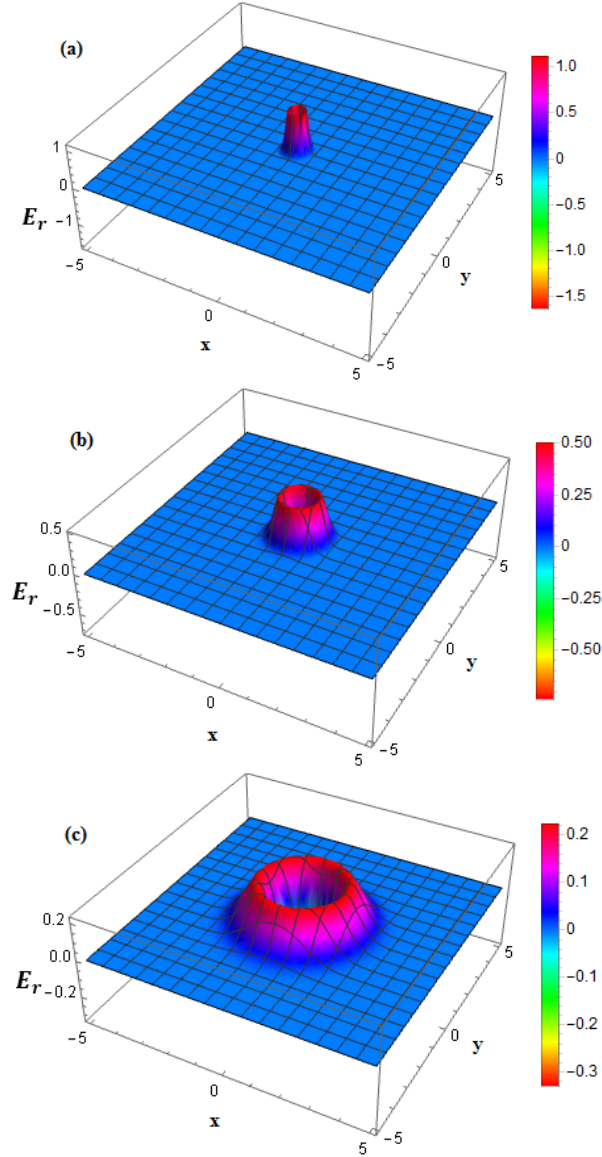
Fig. 2. Radial electric field amplitude associated with LG beam by varying the propagation distance (a) $z = z_R$ (b) $z = 3\,z_R$ (c) $z = 7\,z_R$.

The scattered field distribution depends on LG beam parameters i.e., topological charge (l) and beam waist radius (w_0). The normalized scattered field distribution is plotted against equation (9) and discussed by varying the different influencing factors. On plotting equation (13) of Ref. (Kozaki, 1982) for ($\alpha = 0^0, 90^0$) and also keeping the beam parameters i.e., $p = 0\ \&\ l = 0$ for

different configurations of cylinder (a) PEMC (b) PMC, the scattering behavior of LG_{00} beam and gaussian beam is same. It is observed that scattered field response at $(\alpha = 0^0, 90^0)$ for equation (13) of a gaussian beam of (Kozaki, 1982) coincides with the PEMC cylinder and PMC cylinder of LG_{00} beam. The results are shown in Figure. 3(a) and 3(b) respectively.
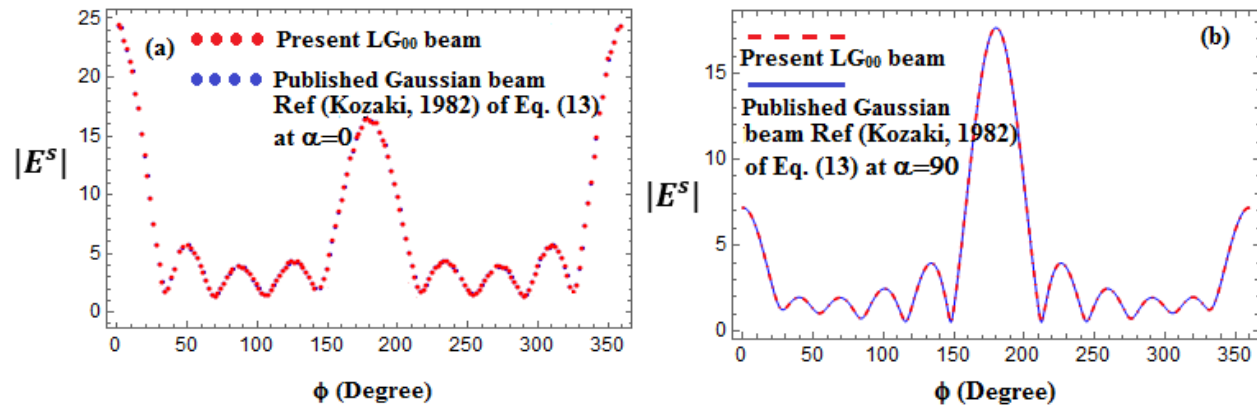
Fig. 3. Comparison of the scattered field of gaussian beam and LG_{00} beam with its mode indices i.e., $p = 0$ and $l = 0$ (a) PEMC cylinder (b) PMC cylinder.

After that we focused to probe the effects of OAM i.e., by varying (l) so, we held the parameter $p = 0$. To layout the effect of the OAM, the scattered field response of LG beam for PEMC cylinder for four feasible cases with different combinations of p and l, that are., (a) $p = 0, l = 1$ (b) $p = 0, l = 2$ (c) $p = 0, l = 3$ and (d) $p = 0, l = 4$ is shown in Fig. 4. For $l = 1, 2$ a smooth field pattern appears in between $\varphi = 0^0 - 150^0$ and $\varphi = 200^0 - 350^0$, but around the center of optical axis i.e., $150^0 - 200^0$, a peak for the scattered field becomes more prominent. Here a sharp hump can be seen. However, the scattered field has maximum value for $l = 4$.
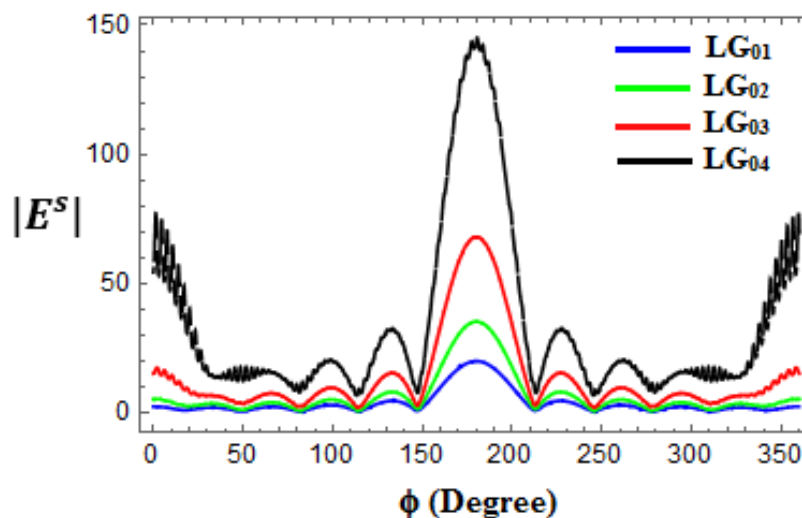
Fig. 4. Scattered field response of LG beam for OAM index $l = 1,2,3,4$ for PEMC cylinder.

The effects of varying the beam waist radius for PEMC cylinder is shown in Figure. 5. The scattered field distribution increases as the waist radius increases. On continuous increasing the waist radius, the size of the hole for the LG beam intensity distribution increases and leads to increase the beam width which in turn increasing the normalized scattered field pattern. The distance among the various peaks becomes shorter due to continuous increasing the waist radius. It seems that field pattern for LG beam increases by increasing the beam waist radius (w_0) as for the gaussian beams.
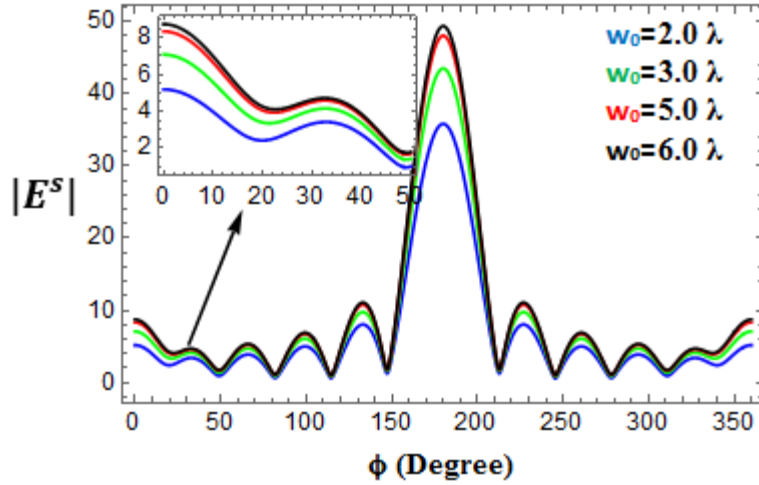
Fig. 5. Scattered field response of *LG* beam for beam waist radius (w_0) for PEMC cylinder.

Figure. 6 shows the scattering behavior of LG beam versus admittance parameter by changing the OAM index. The scattering response increases by increasing the *l* parameter. The RCS for all the other values of admittance parameter show flat response but at the center of the optical axis, a sharp peak appears which corresponds to the more involvement of internal field modes. The central peak size also increases by increasing the OAM mode number. The difference among various peaks increases form minor to major by increasing the beam *l*.
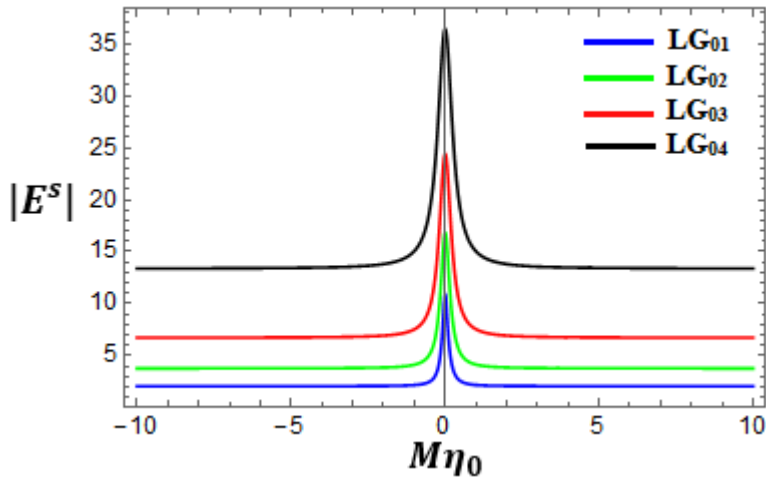
Fig. 6. Scattered field response of *LG* beam versus admittance parameter for PEMC cylinder.

In Figure. 7, the effect of cylinder radius on scattered field has been plotted. The scattered field distribution depends on cylinder radius also. It is clear from the Figure. 7 that when the radius of the cylinder is small the scattered field is small and it increases by increasing the radius. A noticeable pattern is also observed by increasing the cylinder radius. It can be observed that the scattered field for LG incident beam does not always increase with the increase of PEMC cylinder radius. However, there exists an optimum PEMC cylinder size for the maximum scattered field which is also controlled by beam order and beam waist radius.
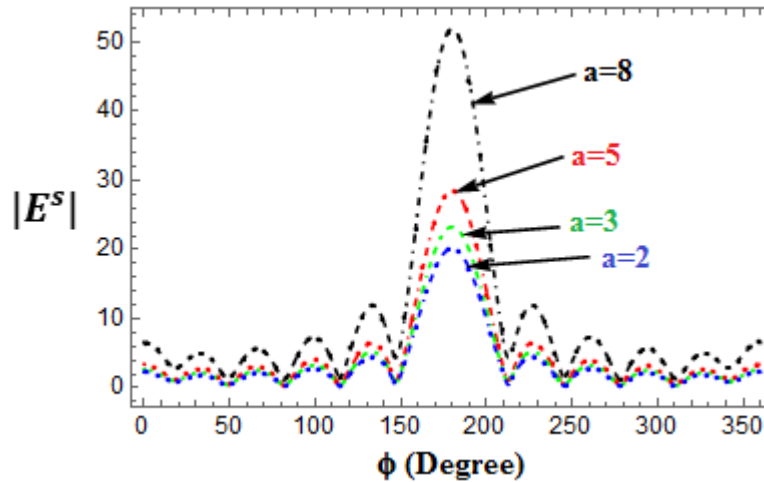
Fig. 7. Scattered field response of *LG* beam for the radius of PEMC cylinder.

4. Conclusions

We have developed an analytical technique to study the scattering field pattern of a PEMC cylinder that is illuminated by an incident LG beam. The field components of LG beam need to be described by mathematical expressions in cylindrical coordinate system. Here, we briefly described an arbitrary incident LG beam by using the method of constructing scalar potential. The present theoretical treatment is considered to be more general for considering any perfect conductor cylinder i.e., (PEC/ PMC/ PEMC). A comparison of the numerical results with the published results under some special case confirm the validity of our analysis. It is concluded that scattered field for PEMC cylinder can be tuned by varying the OAM mode index, beam waist radius, and PEMC cylinder radius.

ACKNOWLEDGMENTS

References

Ahmed, S., Manan, F., Shahzad, A. & Naqvi, Q. A. (2011). Electromagnetic scattering from a chiral-coated PEMC cylinder. Progress In Electromagnetics Research, 19, 239-250.

Arfan, M., Alkanhal, M. A., Ghaffar, A. & Alqahtani, A. H. (2022a). Scattering of Laguerre–Gaussian beam from a chiral-coated perfect electromagnetic conductor (PEMC) cylinder. Journal of Computational Electronics**,** 1-10.

Arfan, M., Ghaffar, A., Alkanhal, M. A., Naz, M., Alqahtani, A. H. & Khan, Y. (2022b). Orbital Angular Momentum Wave Scattering from Perfect Electromagnetic Conductor (PEMC) Sphere. Optik**,** 168562.

Ayub, M., Ali, S. & Mendonca, J. (2011). Phonons with orbital angular momentum. Physics of Plasmas, 18**,** 102117.

Cui, Z., Guo, S., Wang, J., Wu, F. & Han, Y. (2021). Light scattering of Laguerre–Gaussian vortex beams by arbitrarily shaped chiral particles. JOSA A, 38**,** 1214-1223.

Friese, M., Enger, J., Rubinsztein-Dunlop, H. & Heckenberg, N. R. (1996). Optical angular-momentum transfer to trapped absorbing particles. Physical Review A, 54**,** 1593.

Ghaffar, A., Ahmad, S., Fazal, R., Shukrullah, S. & Naqvi, Q. (2013). Scattering of electromagnetic wave by perfect electromagnetic conductor (PEMC) sphere placed in chiral media. Optik, 124**,** 4947-4951.

Jackson, J. D. 1999. Classical electrodynamics. American Association of Physics Teachers.

Kozaki, S. (1982). A new expression for the scattering of a Gaussian beam by a conducting cylinder. IEEE Transactions on antennas and propagation, 30**,** 881-887.

Li, H., Honary, F., Wu, Z. & Bai, L. (2017). Reflection and transmission of Laguerre-Gaussian beams in a dielectric slab. Journal of Quantitative Spectroscopy and Radiative Transfer, 195**,** 35-43.
Lindell, I. V. & Sihvola, A. H. (2005). Transformation method for problems involving perfect electromagnetic conductor (PEMC) structures. IEEE Transactions on antennas and propagation, 53**,** 3005-3011.

Mair, A., Vaziri, A., Weihs, G. & Zeilinger, A. (2001). Entanglement of the orbital angular momentum states of photons. Nature, 412**,** 313-316.

Mendonca, J., Ali, S. & Thidé, B. (2009). Plasmons with orbital angular momentum. Physics of Plasmas, 16**,** 21031-21035.

Qu, T., Wu, Z.-S., Shang, Q.-C. & Li, Z.-J. (2016). Light scattering of a Laguerre–Gaussian vortex beam by a chiral sphere. JOSA A, 33**,** 475-482.

Ruppin, R. (2006a). Scattering of electromagnetic radiation by a perfect electromagnetic conductor cylinder. Journal of Electromagnetic Waves and Applications, 20**,** 1853-1860.

Ruppin, R. (2006b). Scattering of electromagnetic radiation by a perfect electromagnetic conductor sphere. Journal of Electromagnetic Waves and Applications, 20**,** 1569-1576.

Shahzad, K. & Ali, S. (2014). Finite orbital angular momentum states and Laguerre–Gaussian potential in two-temperature electron plasmas. Astrophysics and Space Science, 353**,** 3-8.

Sihvola, A. (2007). Metamaterials in electromagnetics. Metamaterials, 1**,** 2-11.

Sihvola, A. & Lindell, I. V. Possible applications of perfect electromagnetic conductor (PEMC) media. 2006 First European Conference on Antennas and Propagation, 2006. IEEE, 1-4.

Tempere, J., Devreese, J. & Abraham, E. (2001). Vortices in Bose-Einstein condensates confined in a multiply connected Laguerre-Gaussian optical trap. Physical Review A, 64**,** 023603.

Yao, A. M. & Padgett, M. J. (2011). Orbital angular momentum: origins, behavior and applications. Advances in Optics and Photonics, 3**,** 161-204.

Yu, M., Han, Y., Cui, Z. & Sun, H. (2018). Scattering of a Laguerre–Gaussian beam by complicated shaped biological cells. JOSA A, 35**,** 1504-1510.

Zhao, L. & Xie, H. (2016). Interaction between electromagnetic wave and magnetized plasma slab with linearly varying electron density with metallic substrate. Kuwait Journal of Science, 43.